Myeloid cell-restricted Insulin/IGF-1 receptor deficiency protects against skin inflammation

Jana Knuever[#][*], **Sebastian Willenborg**[#][*], **Xiaolei Ding**[*], **Mehmet D. Akyüz**[*,‡], **Linda Partridge**[‡,§], **Carien M. Niessen**[*,‡,¶], **Jens C. Brüning**[‡,¶,‖,†], and **Sabine A. Eming**[*,‡,¶]

[*]Department of Dermatology, University of Cologne, Cologne, Germany

[‡]Cologne Excellence Cluster on Cellular Stress Responses in Aging-Associated Diseases (CECAD), University of Cologne, Germany

[§]Max Planck Institute for Biology of Ageing, Cologne, Germany

[¶]Center for Molecular Medicine Cologne (CMMC), University of Cologne, Germany

[‖]Max Planck Institute for Metabolism Research, Cologne, Germany

[†]Center for Endocrinology, Diabetes and Preventive Medicine (CEDP), University Hospital Cologne, Cologne, Germany

[#] These authors contributed equally to this work.

Abstract

Myeloid cells are key regulators of tissue homeostasis and disease. Alterations in cell-autonomous Insulin/IGF-1 signaling in myeloid cells have recently been implicated in the development of systemic inflammation and insulin-resistant diabetes mellitus type 2 (DM). Impaired wound healing and inflammatory skin diseases are frequent DM-associated skin pathologies, yet the underlying mechanisms are elusive. Here we investigated whether myeloid cell-restricted IR/IGF-1R signalling provides a pathophysiological link between systemic insulin resistance and the development of cutaneous inflammation. Therefore, we generated mice lacking both the Insulin and IGF-1 receptor in myeloid cells (IR/IGF-1R^{MKO}). Whereas the kinetics of wound closure following acute skin injury was similar in control and IR/IGF-1R^{MKO} mice, in two different conditions of dermatitis either induced by repetitive topical applications of the detergent SDS or by high-dose UVB radiation, IR/IGF-1R^{MKO} mice were protected from inflammation, whereas controls developed severe skin dermatitis. Notably, whereas during the early phase in both inflammatory conditions the induction of epidermal pro-inflammatory cytokine expression was similar in control and IR/IGF-1R^{MKO} mice, during the late stage, epidermal cytokine expression was sustained in controls, however virtually abrogated in IR/IGF-1R^{MKO} mice. This distinct kinetic of epidermal cytokine expression was paralleled by pro-inflammatory macrophage

activation in controls and a non-inflammatory phenotype in mutants. Collectively, our findings provide evidence for a pro-inflammatory IR/IGF-1R-dependent pathway in myeloid cells that plays a critical role in the dynamics of an epidermal-dermal crosstalk in cutaneous inflammatory responses, and may add to the mechanistic understanding of diseases associated with disturbances in myeloid cell IR/IGF-1R signaling including DM.

Introduction

Myeloid cells have been identified as critical regulators of a variety of inflammatory, hormonal and metabolic processes in different organ and model systems (1, 2). A typical feature of monocytes/macrophages is their broad phenotypic and functional plasticity, and their function as sensors and effectors of a specific microenvironment (3). Yet, which specific mediators and signals control monocyte/macrophage function in defined local tissue microenvironments is largely unknown. A better understanding of how macrophage plasticity and function is controlled would provide further insight into their impact on systemic and local, organ specific inflammation. Therefore, it will be important to identify specific factors that may direct monocyte/macrophage function on a tissue and systemic level because these insights may open up new avenues to monitor disease progression and potentially for pharmacological control of monocyte/macrophage function.

Recent experimental evidence suggests that alterations in cell-autonomous Insulin/IGF-1 signaling in myeloid cells play a pivotal role in the development of obesity-induced inflammation, systemic insulin resistance and insulin-resistant diabetes mellitus type 2 (DM) associated vascular disease (4, 5). Thus, myeloid insulin sensitivity may provide the critical link between systemic insulin resistance and DM associated organ specific diseases. DM represents a frequent endocrine disease, currently with a prevalence of 6.4% in the world population and anticipated increase close to 8% in the year 2030 (6). The skin is one of the organs frequently affected in DM contributing to morbidity and mortality. Common DM-associated skin complications include impaired wound healing, cutaneous infections, xerosis, pruritus, psoriasis, and other less well defined pro-inflammatory alterations (7-9). The underlying mechanisms are not resolved, and specific and effective therapeutic interventions are lacking. Besides the direct consequences of the disturbed glucose metabolism, insulin/IGF-1 resistance on a cell/tissue-autonomous level may contribute to the development and/or progression of skin disorders in DM (10-16). Furthermore, based on the reported critical role of Insulin- (IR) receptor activation in cells of the myeloid lineage in chronic adipose tissue inflammation (5), it is intriguing to speculate that alterations in IR/IGF-1R mediated myeloid cell activation directly contribute to diabetes associated regenerative and/or inflammatory skin complications.

Up to date the specific role of the IR/IGF-1R in myeloid cell function has been little investigated. Early studies demonstrated that monocytes/macrophages express the IR (17) and that they respond to Insulin with increased phagocytosis and glucose metabolism (18). Furthermore, Insulin and IGF-1 have been reported to be potent inducers of TNF-α synthesis in murine and/or human macrophages (19). Consistent with a pro-inflammatory role of Insulin/IGF-1 action in macrophages is the observation that myeloid cell-restricted IR

deficiency protects mice against atherosclerosis or obesity-induced inflammation and systemic insulin resistance (4, 5). In this study, we explored the role of myeloid cell-restricted Insulin and Insulin-like growth factor 1 (IGF-1) signaling in cutaneous wound healing and diverse models of skin inflammation.

Insulin and IGF-1 are central mediators of a multitude of metabolic, growth and survival activities. Both factors mediate their functions through binding with different affinities to the IR and/or IGF-1R that are widely expressed on different cell types in diverse tissues (20). Dissecting specific cellular activation through the IR and/or IGF-1R by Insulin and/or IGF-1 is complicated by the fact that both receptors form diverse hybrids which bind their ligands with different affinities (21). To address the complexity of IR/IGF-1R signaling and to assure efficient abrogation of both ligand/receptor systems we generated mice lacking both the IR and the IGF-1R in myeloid cells (IR/IGF-1R^{MKO}) and exposed mutant and control mice to cutaneous acute and prolonged stress responses. Our findings provide novel mechanistic insights into an important crosstalk between epidermal and myeloid cells that is controlled by myeloid cell-restricted IR/IGF-1R activation. Our findings may be relevant for novel, monocyte-targeted therapies to prevent skin inflammation and/or diabetes mellitus associated skin complications.

Materials and Methods

Animals

Generation of the IR floxed and IGF-1R floxed mouse lines have been described previously (12, 22). To generate mice with myeloid cell-restricted IR and IGF-1R gene deletion, IR$^{fl/fl}$/IGF-1R$^{fl/fl}$ mice were bred to LysMCre mice expressing Cre recombinase under control of the lysozyme M promoter (23) (IR/IGF-1R^{MKO}); IR$^{fl/fl}$/IGF-1R$^{fl/fl}$ mice were used as controls. All mice used in experiments were in C57BL/6 background. Cre-mediated recombination was verified by PCR analysis in genomic DNA as described previously (12, 22). Mice were maintained and bred under standard pathogen-free conditions. Eight- to 12-week-old male mice were used for the experiments. All procedures were in accordance with institutional guidelines on animal welfare and were approved by the North Rhine-Westphalia State Environment Agency, Germany.

Cell culture

Peritoneal cells were seeded in 6-well plates (0.5×10^6 cells/cm^2), macrophage enriched by plastic adhesion in DMEM (10% FCS), serum-starved for 6 h in DMEM and stimulated with a mixture of recombinant mouse Insulin (50 ng/mL; CellSystems, Troisdorf, Germany) and recombinant mouse IGF-1 (50 ng/mL; eBioscience, San Diego, CA, USA) in DMEM for 3 h; gene expression was analyzed by qRT-PCR as described below and phosphorylation of proteins was performed using the commercially available PathScan® Intracellular Signaling Array Kit as described below; macrophages grown in DMEM served as controls.

PathScan® Intracellular Signaling Array Kit (Chemiluminescent Readout)

Cell lysates were prepared by the manufacturer's instructions and applied with a total protein concentration of 0.2 mg/mL to the membrane. The array (Cell Signaling Technology,

Beverly, MA, USA) was performed according to the manufacturer's recommendations. The chemiluminescent reaction was depicted with an ImageQuant LAS 4000 Mini (GE Healthcare Life Sciences, Pittsburgh, PA, USA). The pictures were analyzed by Dot Blot Analysis, Image J (http://rsb.info.nih.gov/ij/docs/examples/dot-blot/index.html). Intensity values of the stimulated lysates were normalized to non-stimulated controls.

SDS-PAGE Immunoblotting

To analyze IR and IGF-1R gene deletion efficiency peritoneal macrophages were enriched by plastic adhesion, cell lysates were resolved on a 4-12% reducing BisTris SDS-PAGE gel (NUPAGE, Invitrogen) and transferred to a nitrocellulose membrane (Hybond C-extra, Amersham Biosciences). Immunoreactive products were detected using the following primary antibodies: rabbit anti-IGF-1Rβ (C-20), rabbit anti-IRβ (C-19) (Santa Cruz Biotechnology, Santa Cruz, CA, USA), mouse anti-α-Tubulin (Sigma-Aldrich, St. Louis, MO, USA). Phosphorylation of proteins were detected in lysates and resolved in SDS-PAGE gel as described above; primary antibodies included rabbit anti-p38α MAPK, rabbit anti-phosphop38α MAPK$^{T180/Y182}$, rabbit anti-Akt, rabbit anti-phospho-Akt^{S473}, rabbit anti-phospho-Akt^{T308} (Cell Signaling Technology, Beverly, MA, USA), mouse anti-GAPDH (Calbiochem, La Jolla, CA, USA), mouse anti-α-Tubulin. Bound primary antibody was detected using a rabbit anti-mouse HRP-conjugated secondary antibody and a swine anti-rabbit HRP-conjugated antibody (Dako, Glostrup, Denmark). Detection of bound secondary antibody was accomplished using the enhanced chemiluminescence Western blot detection system ECL (Perkin Elmer, Waltham, MA, USA).

Flow cytometric analysis and cell sorting

Blood monocytes and skin macrophages were isolated and prepared for FACS analysis as described recently (32). Briefly, blood monocytes were isolated from heparinized blood by hypotonic lysis of erythrocytes using red blood cell lysis solution (Miltenyi Biotec, Bergisch Gladbach, Germany), followed by ice-cold PBS (1% BSA and 2 mM EDTA) washes. Macrophages were isolated from skin following a combination of enzymatic digestion with Liberase Blendzyme (Roche Applied Science, Penzberg, Germany) and mechanical disruption using the Medimachine System (BD Biosciences, San Jose, CA, USA). Thioglycolate-elicited peritoneal macrophages were isolated 4 days after a single injection of 4% thioglycolate (Sigma-Aldrich) by peritoneal lavage using 8 mL PBS (1% BSA and 2 mM EDTA). For FACS analysis, Fc receptors were blocked with mouse seroblock FcR (CD16/CD32) and cells were stained with PE-conjugated anti-F4/80 (AbD Serotec, Oxford, UK), APC-conjugated anti-CD11b (Miltenyi Biotec), PE-Cy7-conjugated anti-Ly6C (BD Biosciences), FITC-conjugated anti-CD45, APC-Cy7-conjugated anti-Ly6G, APC-conjugated anti-CD115 (eBioscience). The following isotype controls were used: FITC-conjugated rat IgG2a, PE-conjugated rat IgG2b, APC-conjugated rat IgG2b (eBioscience) and PE-Cy7–conjugated rat IgM (BD Biosciences). Cells were incubated with antibodies for 20 min at 4°C and washed 3 times thereafter in washing buffer (1% BSA and 2 mM EDTA in PBS). Dead cells were excluded using 7-amino-actinomycin D (BD Biosciences). Cells were analyzed using a FACSCanto II flow cytometer or sorted using a FACSAria III cell sorter using FACSDiva Version 6.1.1 (BD Biosciences).

Wounding, SDS treatment, UVB irradiation and preparation of tissues

Wounding was performed as recently described (32). Briefly, mice were anaesthetized, shaved and four full-thickness punch biopsies were created on the back. For UVB irradiation and SDS treatment mice were anaesthetized and the shaved back was exposed to a single UVB irradiation (area of 2 cm^2, dose of 600 mJ/cm^2, UV device: TP-4, Waldmann, UV-6 lamps) or painted daily for 3 or 6 days with SDS (5% in PBS; 0.5 mL applied on area of 2 cm^2) (24-26). For histological analysis and RNA isolation, mice were sacrificed at indicated time points and wounds or treated skin were excised, bisected in the caudocranial direction, and the tissue was fixed in 4% formaldehyde, embedded in optimal cutting temperature compound Tissue-Tek (Miles Scientific, IL, USA) or stored in RNAlater® solution (Life Technologies). SDS-treated skin was separated into epidermal and dermal tissue by trypsin incubation (0.5%, 1 h at 37°C) and processed for RNA isolation and real-time PCR analysis as described below.

Real-time PCR analysis

RNA from UV-irradiated or SDS-treated skin was isolated using the Fibrous Tissue Mini Kit (Qiagen, Hilden, Germany) and RNA from single-cell suspensions was isolated using the RNeasy Micro Kit (Qiagen, Hilden, Germany) according to the manufacturer's instructions. Reverse transcription of isolated RNA was performed using the High Capacity cDNA RT Kit (Life Technologies, Gaithersburg, MD, USA). Primers (Sigma-Aldrich) were generated as outlined in Supplemental Table I. Amplification reactions (triplicates) were set up using PowerSYBR Green PCR Master Mix (Life Technologies) and quantitative RT-PCR (qRTPCR) was validated with the 7300 Real Time PCR system (Life Technologies). The comparative method of relative quantification ($2^{-\Delta Ct}$) was used to calculate the expression level of the target gene normalized to GAPDH. The amplified PCR fragments were a maximum of 250 bp in length and the annealing temperature was 60°C.

Immunohistochemistry

Immunohistochemical stainings (10 μm cryosections) were performed as described previously (31, 32). Bound primary antibodies (anti-CD68, AbD Serotec; anti-Ki67, Dako) were detected by incubation with an Alexa Fluor 488-conjugated secondary antibody (Invitrogen), followed by counterstaining with DAPI or Propidium Iodide (Life Technologies); anti-Gr-1 (BD Biosciences) immunostaining was performed using a peroxidase detection system and hematoxylin counter stain. Specificity of primary antibodies was demonstrated by replacing them with irrelevant isotype-matched antibodies.

Morphometric analysis

Morphometric analysis was performed on H&E-stained paraffin tissue sections using light microscopy equipped with a KY-F75U digital camera (JVC) at 10x magnification (Leica DM4000B, Leica Microsystems; Diskus 4.50 Software, Diskus) (31, 32). Epidermal thickness was measured in several points over the entire length of the SDS-treated or UV-exposed area at a distance of 25 μm and the mean was calculated. Counts of mast cells (Giemsa stain) or Gr-1$^+$ cells were acquired in high-power fields (450 μm × 360 μm) using Leica light microscopy (objective: 20x, NA 0.4). CD68$^+$ or Ki67$^+$ cells were quantified in

high-power fields (400 μm × 315 μm) using a Nikon Eclipse 800E microscope (NIS-Elements AR 2.30 software, DXM 1200F digital camera) and ImageJ software (objective: 20x, NA0.75). The proportion of proliferating keratinocytes was analyzed by counting Ki67$^+$ cells within the basal layer of the epidermis over a length of 300 μm. Analyses were performed in a blinded manner by 2 independent investigators. Images were processed with Adobe Photoshop Version 7.0 software.

Statistical analysis

Statistical analyses were performed using Prism Version 5 software (GraphPad, San Diego, CA, USA). Significance of difference was analyzed with a Student paired or unpaired 2-tailed *t* test and ANOVA 1-way test analysis. In cases of variances that were not assumed to be equal, a Welch correction was performed. $P < 0.05$ was considered significant (*$p < 0.05$, **$p < 0.01$, ***$p < 0.001$).

Results

Generation of mice with myeloid cell-restricted Insulin and IGF-1 receptor deletion

To examine the role of myeloid cell-specific Insulin/IGF-1 signaling, we generated mice that lack both the Insulin and IGF-1 receptor in myeloid cells. Therefore, we crossed the previously generated IR$^{fl/fl}$ (22) and IGF-1R$^{fl/fl}$ (12) mouse lines with LysMCre (23) mice to create myeloid cell-specific IR and IGF-1R knock-out mice (IR/IGF-1R^{MKO}). Cre-mediated recombination deletes exon 4 and exon 3 of the IR and IGF-1R gene, respectively. Cre-mediated gene deletion was verified by PCR analysis of genomic DNA extracted from peritoneal macrophages (Fig. 1A) and deletion efficiency was proven by Western Blot analysis for IR and IGF-1R (Fig. 1B). IR/IGF-1R^{MKO} mice were born in the expected Mendelian ratio and developed normally without any obvious phenotype.

Myeloid cell-restricted IR/IGF-1R deletion does not cause major alterations in wound closure kinetics but attenuates formation of granulation tissue

To investigate whether loss of IR/IGF-1R in myeloid cells would affect skin wound healing, full-thickness skin wounds were inflicted on the backs of control and IR/IGF-1R^{MKO} mice. Macroscopic appearance of wound closure was similar in control and IR/IGF-1R^{MKO} mice (Supplemental Fig. 1A). Quantitative analysis of haematoxylin-eosine stained wound sections at early (day 4), mid (day 7) and late (day 14) stages of the repair response showed a significant reduction in granulation tissue at day 7 post injury in IR/IGF-1R^{MKO} mice compared to controls (Supplemental Fig. 1B). However, overall kinetics of wound closure (measured by the distance between epithelial tips and the length of the epithelial tongues), vascularization (CD31 staining), formation of myofibroblasts (αSMA-staining) and the density of macrophages (F4/80 staining) within the granulation tissue were similar in control and IR/IGF-1R^{MKO} mice (Supplemental Fig. 1B, C). As assessed by qRT-PCR analysis of wound tissue, gene expression of both IGF-1 and -2 was similar in control and IR/IGF-1R^{MKO} mice (Supplemental Fig. 2). Together, these findings suggest that IR/IGF-1R signaling in myeloid cells is dispensable in skin re-epithelialization and wound contraction.

Myeloid cell-specific IR/IGF-1R deficiency protects against SDS-induced skin inflammation

The reported critical importance of IR signaling in myeloid cells for the establishment of a chronic pro-inflammatory state during the course of obesity-induced inflammation and development of DM (5), prompted us to examine the role of myeloid cell-restricted IR/IGF-1R function in a model of a more sustained skin inflammatory response. For this purpose we used a model of irritant contact dermatitis in which sodium dodecylsulfate (SDS 5%) is repeatedly applied topically on a daily base for 6 consecutive days on the shaved back skin of IR/IGF-1R^{MKO} and control mice (24). Detergent-mediated disruption of epidermal barrier function has been reported earlier to induce pro-inflammatory cytokine synthesis causing leukocyte infiltration, acanthosis and hyperkeratosis (24-26). Control mice presented with an erythema starting at day 4 post-treatment, which increased in severity over the following 3 days and at day 7 was characterized by skin thickening, scales and erosions (Fig. 2A). In contrast, SDS-treated skin in IR/IGF-1R^{MKO} mice did not develop obvious macroscopic signs of irritation including erythema and/or scaliness.

Histological analysis of SDS-treated skin tissue was consistent with macroscopic findings. Whereas the epidermis in skin lesions 4 days post SDS treatment in control and mutant mice showed a comparable, modest increase in acanthosis, at day 7 post SDS treatment acanthosis and hyperkeratosis further increased in controls however remained at a modest level in IR/IGF-1R^{MKO} mice (Fig. 2B). Acanthosis at day 4 post SDS treatment in control and mutant mice was caused by an increase in keratinocyte proliferation as revealed by a significant increase of Ki67$^+$ cells within the stratum basale. However, whereas in controls at day 7 post SDS treatment the fraction of Ki67$^+$ cells remained increased, in mutant mice the number of Ki67$^+$ cells declined to normal levels similar in untreated skin (Fig. 2B). Furthermore, 4 days post SDS treatment lesions in control and mutant mice showed a significant increase of leukocyte infiltration when compared to untreated skin, which was characterized by increased numbers of polymorphonuclear cells (Gr-1$^+$ cells) and macrophages (CD68$^+$ cells). Of note, whereas in control mice the increased leukocyte cell infiltrate was sustained until day 7 post SDS treatment, in mutant mice the number of both polymorphonuclear cells and macrophages declined to levels of untreated skin (Fig. 2B). Reduced numbers of leukocytes in skin lesions of IR/IGF-1R^{MKO} mice did not result from a reduction of circulating blood monocytes (SSC^{low}CD11b$^+$CD115$^+$ cells), as numbers of those were similar in mutants and controls (data not shown).

Dynamics of epidermal cytokine expression are associated with myeloid cell-specific IR/IGF-1R activation

To determine how myeloid cell-specific IR/IGF-1R activation impacts the temporal expression of pro-inflammatory mediators in the epidermal and/or dermal compartment of the skin upon SDS treatment, we isolated RNA separately from the epidermis and dermis at several time points during the early (6 hours until 24 hours) and late phase (day 4 and 7) of SDS treatment, and performed qRT-PCR analysis. Interestingly, no difference in induction of pro-inflammatory cytokines and chemokines expression was observed in the epidermis of control and IR/IGF-1R^{MKO} mice during the early phase of SDS treatment (Fig. 3). In fact, in control and mutant mice as early as 6 hours after the first SDS application a pronounced increase of the pro-inflammatory cytokines IL-6, IL-1β and TNFα was detected in

epidermal tissues, whereas epidermal expression of the chemokines MIP1α, MCP-1 and MCP-3 was somewhat delayed and started to be detectable 24 h after treatment. Strikingly, during the late phase of SDS treatment at day 4 and 7, expression levels of pro-inflammatory cytokines and chemokines rapidly declined to barely detectable levels in mutants (except for CXCL1, Supplemental Fig. 1D), whereas expression was sustained in controls (except for IL-6).

In the dermal compartment of control and mutant mice, expression of pro-inflammatory cytokines and chemokines was low or virtually absent during the early phase of SDS treatment. Notably, whereas in controls during the late phase of SDS treatment expression levels of pro-inflammatory cytokines and chemokines in the dermis significantly increased, they remained low in mutant mice (Fig. 3). Also of interest, in controls gene expression of the immunosuppressant IL-10 was barely regulated in epidermal and dermal tissues, however in IR/IGF-1R^{MKO} mice IL-10 was significantly increased at day 4 in the dermis and at day 7 in the epidermis. Collectively, these findings suggest a timely controlled cross-talk between epidermis and myeloid cells that is tightly controlled by IR/IGF-1R expression in myeloid cells.

SDS treatment induces IGF-1 expression in the epidermis and dermis

To further examine whether the delayed induction of pro-inflammatory mediators within the dermal compartment in IR/IGF-1R^{MKO} mice is associated with an altered gene expression of the IR/IGF-1R ligands IGF-1 and IGF-2, we evaluated RNA expression dynamics of both ligands. SDS treatment induced a robust and sustained induction of IGF-1 expression in both epidermis and dermal tissue, whereas upregulation of IGF-2 was modest (Fig. 4). Levels and kinetics of expression of both IGFs increased over time during SDS treatment and were comparable in control and IR/IGF-1R^{MKO} mice.

Myeloid cell-specific IR/IGF-1R expression controls the activation phenotype of macrophages

Whereas during the early phase of SDS-induced skin inflammation (day 4) the density of the leukocyte cell infiltration was similar in control and IR/IGF-1R^{MKO} mice, during the late stage of SDS treatment (day 7) histological analysis revealed a significant attenuation of polymorphonuclear leukocyte and macrophage infiltration in mutant versus control mice (Fig. 2B). These findings suggest that the cell migratory ability or chemotaxis of myeloid cells in mutant mice is not majorly affected. Consistently, elicitation of peritoneal macrophages (CD45$^+$CD11b$^+$F4/80$^+$Ly6C$^+$) by a single intraperitoneal thioglycolate injection was comparable in control and mutant mice (Supplemental Fig. 3). Thus, we next asked whether macrophage activation might be altered as a consequence of IR/IGF-1R deficiency. Consistent with the histological analysis, FACS analysis of single cell suspensions isolated from SDS treated skin revealed that there was a significant increase in polymorphonuclear leukocyte number in controls, which was virtually absent in skin of IR/IGF-1R^{MKO} mice (Fig. 5A). Furthermore, the CD45$^+$CD11b$^+$Ly6G$^-$ fraction was gated for the pro-inflammatory marker Ly6C which defines inflammatory monocytes/macrophages. Notably, in control skin the fraction of inflammatory CD45$^+$CD11b$^+$Ly6G$^-$Ly6C^{hi} cells was significantly increased compared to non-inflammatory CD45$^+$CD11b$^+$Ly6G$^-$Ly6C^{lo} cells,

whereas in SDS-treated skin in IR/IGF-1R^{MKO} mice the balance between these two macrophage populations is shifted almost completely to the non-inflammatory CD45$^+$CD11b$^+$Ly6G$^-$Ly6C^{lo} phenotype (Fig. 5A). Collectively, these findings indicate that loss of IR/IGF-1R responsiveness in monocytes/macrophages disturbs the balance between pro-inflammatory and non-inflammatory macrophages/monocytes causing a shift towards an attenuation of the pro-inflammatory and an induction of the non-inflammatory macrophage phenotype. In accordance with this assumption, CD45$^+$CD11b$^+$Ly6G$^-$Ly6C^{hi} cells of SDS-treated skin in controls were characterized by high expression of TNFα and iNOS, whereas expression of these genes was almost absent in IR/IGF-1R^{MKO} mice and comparable to levels detected in CD45$^+$CD11b$^+$Ly6G$^-$Ly6C^{lo} cells of controls and circulating blood monocytes (SSC^{low}CD115$^+$CD11b$^+$) FACS sorted from non-treated control and mutant mice (Fig. 5B). Of note, in SDS-treated skin in IR/IGF-1R^{MKO} mice Relm-α, a marker of alternative (non-inflammatory) macrophage activation, was significantly increased in Ly6C^{lo} cells when compared to SDS-treated skin in controls (Fig. 5B).

Myeloid cell-specific IR/IGF-1R deficiency protects from UVB light-induced skin inflammation

To substantiate our findings of a critical pro-inflammatory role in myeloid cell-restricted Insulin/IGF-1 in skin inflammation, we examined the cutaneous response of UVB light exposure in IR/IGF-1R^{MKO} mice, which provides a more natural pro-inflammatory stimulus for the skin. The effect of UV irradiation in skin inflammation is complex and known to induce dose-dependent early (< 24 hours) and late (2-7 days) immune-modulating events (27). Here, we assessed whether myeloid cell-restricted IR/IGF-1R deficiency impacts the UVB light-induced late stage pro-inflammatory response (day 7) upon exposing control and IR/IGF-1R^{MKO} mice to a single, high dose of UVB light. As expected, control mice presented with an erythema, scales and thickening of UV-treated skin (Fig. 6A). In contrast, the skin of UV-treated IR/IGF-1R^{MKO}mice appeared macroscopically normal. Consistent with reported histological alterations at late-stage UVB exposure (27), 7 days after irradiation skin of control mice was characterized by acanthosis, hyperkeratosis and by a mixed leukocyte infiltrate composed of a significantly increased number of macrophages (F4/80$^+$ cells), polymorphonuclear leukocytes (Gr-1$^+$ cells) and mast cells (Giemsa stain) when compared to non-exposed controls (data not shown). In contrast, although in IR/IGF-1R^{MKO} mice epidermal thickness of irradiated skin was increased when compared to non-irradiated mice, the acanthosis and hyperkeratosis were significantly less pronounced when compared to irradiated controls (Fig. 6A). As revealed by FACS analysis of single cell suspensions isolated from skin 7 days after UVB exposure and histological analysis of tissue sections (data not shown), the number of different leukocyte subsets (F4/80$^+$ cells, polymorphonuclear leukocytes, mast cells) was similar in control and IR/IGF-1R^{MKO} mice (Fig. 6B).

To assess macrophage activation after UVB exposure, gene expression of monocytes/ macrophages in irradiated lesions was correlated with gene expression in circulating blood monocytes (SSC^{low}CD115$^+$CD11b$^+$) FACS sorted from non-irradiated mice. Macrophages (CD45$^+$CD11b$^+$F4/80$^+$) in irradiated skin of control mice were characterized by high expression of inflammatory mediators such as TNFα, IL-6 and Il-1β but also the anti-

inflammatory mediator IL-10 (Fig. 6C). Notably, in macrophages of IR/IGF-1R[MKO] mice expression of pro-inflammatory cytokines was significantly reduced whereas IL-10 was significantly upregulated when compared to controls (Fig. 6C). Collectively, these findings indicate that IR/IGF-1R signaling in myeloid cells contributes to the UVB light-induced late stage skin inflammation.

Myeloid cell-specific IR/IGF-1R activation induces a pro-inflammatory macrophage phenotype in vitro and is associated with activation of Akt and p38α MAPK

To identify signaling pathways regulating the inflammatory phenotype of macrophages in response to Insulin/IGF-1, peritoneal macrophages were stimulated with a mixture of recombinant Insulin and IGF-1 for 3 h after which gene expression was analyzed by qRTPCR analysis. Numerous pro-inflammatory mediators were significantly upregulated in control cells upon Insulin/IGF-1 stimulation including TNFα, IL-6, IL-1β, iNOS (Fig. 7A) that were also upregulated *in vivo* in control mice upon SDS treatment or UVB radiation. Notably, also IL-10 was upregulated in control cells. The induction of these genes was virtually absent in IR/IGF-1R deleted macrophages, showing that their expression was a direct result from a loss of IR/IGF-1R signaling.

To identify the key mediators downstream of IR/IGF-1R receptors that control inflammatory response in macrophages, we stimulated isolated peritoneal macrophages of control and IR/IGF-1R[MKO] mice with Insulin/IGF-1 and subjected these to an intracellular signaling array. Insulin/IGF-1 induced a pronounced phosphorylation of Akt^{S473}/Akt^{T308}, p38α$^{T180/Y182}$ and Erk1/2$^{T202/Y204}$ in control but not IR/IGF-1R knockout macrophages, whereas activation of mTOR appeared not to be affected, and pro-apoptotic markers such as caspase 3 were down-regulated (Fig. 7B). To substantiate these findings of down-stream activated components in Insulin/IGF-1 stimulated macrophages we performed Western Blot analysis for selected factors. This confirmed the Insulin/IGF-1 dependent increase in phosphorylation of Akt^{S473}/Akt^{T308} and the stress MAP kinase p38α (Fig. 7C) whereas mTOR activation was not directly regulated by this treatment (data not shown).

Discussion

In this study we reveal a critical role for Insulin/IGF-1 signaling in myeloid cells in skin homeostasis. Our findings provide evidence that myeloid cell-restricted IR/IGF-1R function in skin is context-dependent and varies regarding the nature of the cutaneous stress response. Furthermore, our study indicates that myeloid cell-restricted IR/IGF-1R activation, which has been directly linked to the development of systemic inflammation and DM, also plays a crucial role in the development of skin inflammation. Thus, IR/IGF-1R signalling in myeloid cells may provide a functional link between DM and DM-associated inflammatory skin diseases.

One of the major and still unresolved skin complications associated with type 2 diabetes is impaired wound healing (7). Although it is well accepted that the pathophysiology of chronic wounds in diabetic patients is multifactorial including disturbed inflammatory processes, the exact impact of the perturbed inflammatory response in diabetes impaired healing is still under debate (15, 16, 28-30). Specifically, it is unresolved to which extent

perturbed inflammatory repair processes may be a consequence of the disturbed glucose metabolism and/or may be due to cell autonomous effects of IR/IGF-1R responsiveness in skin resident cells and/or recruited leukocytes. Previously, our groups and others have unravelled important cell type-specific IR/IGF-1R functions on epidermal morphogenesis (12, 13) and on the vascular system (14) both of which are likely to contribute to skin complications in diabetic patients. Furthermore, we and others provided evidence that recruitment and activation of monocytes/macrophages is a pivotal process to assure a timely wound healing response (28-32). Based on the described stimulatory effects of IR on phagocytosis, metabolic and pro-inflammatory activities in macrophages (4, 5), we investigated the hypothesis that myeloid cell-restricted IR/IGF-1R resistance contributes to impaired immune functions and ultimately a disturbed healing response. Here we show that although the amount of granulation tissue deposition was temporarily reduced in IR/IGF-1R^{MKO} mice when compared to controls, the overall kinetics of wound closure following skin injury were similar in mutants and controls. These findings were unexpected and indicate a minor role of myeloid cell-specific IR/IGF-1R signaling in re-epithelialization and wound contraction following acute mechanical injury in otherwise healthy conditions. Nevertheless, at this stage our findings do not exclude that IR/IGF-1R function in myeloid cells becomes critical in the context with other comorbidities that characterize diabetic patients such as arterial disease, neuropathy, obesity, and/or hyperglycemia, and this possibility merits future investigation.

Mice with myeloid cell-restricted IR/IGF-1R deficiency were effectively protected from late stage skin inflammation in response to stimuli that provoke a rather sustained inflammatory response such as repeated topical treatment with SDS or a single, high dose UVB-light exposure. These findings strongly indicate a direct role of Insulin/IGF-1 in myeloid cell function in the development of skin inflammation. The hypothesis of Insulin/IGF-1 signaling being involved in processes of chronic skin inflammation is supported by earlier observations by Partridge and colleagues in complete insulin receptor substrate-1 (IRS-1) deficient mice, which are fully protected from age-associated ulcerative dermatitis (33).

Here we show that induction or rather attenuation of skin inflammation in control and IR/IGF-1R^{MKO} mice, respectively, was associated with a specific expression pattern of pro-inflammatory mediators in the epidermal and dermal compartment in time and space. Whereas within 6 hours following the initial SDS treatment in both IR/IGF-1R^{MKO} and control mice an early and effective induction of potent pro-inflammatory mediators was specifically detected in the epidermis, at later stages at day 4 and 7 expression of these epidermal pro-inflammatory cytokines was significantly reduced in IR/IGF-1R^{MKO} mice when compared to their sustained expression in controls. In the dermal compartment expression of inflammatory cytokines was virtually absent until 24 hours post SDS treatment in both control and mutant mice. However, in controls dermal expression of pro-inflammatory cytokines significantly increased at day 4 and 7, whereas it remained low in IR/IGF-1R^{MKO} mice. Collectively, these findings suggest that upon SDS treatment the epidermis releases early pro-inflammatory mediators that recruit circulating myeloid cells from the blood and that their activation through IR/IGF-1R signaling perpetuates the epidermal and dermal inflammatory response (Fig. 8). Consistent with this assumption is the delayed expression of epidermal IGF-1 at day 4 and 7 which most likely serves to activate

myeloid cells that have been recruited to the dermis through early expression of epidermal pro-inflammatory cytokines such as IL-6 and IL-1β, and potent chemokines.

Myeloid cell-deficiency of IR/IGF-1R did not only reduce the absolute cell number of myeloid cells in the SDS-treated skin, but interestingly also caused a shift in the balance between pro- (CD45^{+}CD11b^{+}Ly6G^{−}Ly6C^{hi}) and non-inflammatory (CD45^{+}CD11b^{+}Ly6GLy6C^{lo}) macrophage phenotypes within the SDS-treated skin lesions towards a predominance of the non-inflammatory phenotype in IR/IGF-1R[MKO] mice. Thus, it is likely that the release of pro-inflammatory mediators from macrophages in control mice contributes to skin inflammation and their absence in IR/IGF-1R[MKO] mice prevents sustaining the initial SDS-induced epidermal inflammatory response in these mice. Notably, the fraction of non-inflammatory macrophages (CD45^{+}CD11b^{+}Ly6G^{−}Ly6C^{lo}) was significantly increased in IR/IGF-1R[MKO] mice when compared to controls and showed the induction of Relm-α (also known as M2 marker associated with alternative macrophage activation). The biological function of Relm-α is not entirely understood, both pro- but also anti-inflammatory activities have been described (34, 35). Therefore, at this stage we cannot exclude that in addition to the lack of the induction of a pro-inflammatory macrophage phenotype, also the induction of an alternative/anti-inflammatory activated phenotype contributes to the protection of IR/IGF-1R[MKO] mice to skin inflammation. Overall, these findings strongly support the concept that IR/IGF-1R activation in monocytes/macrophages controls the balance between pro- and non-inflammatory macrophage populations during development of skin inflammation.

Our findings of a pro-inflammatory function of IR/IGF-1R in myeloid cells in skin homeostasis were highlighted by the observation that IR/IGF-1R[MKO] mice were also protected from UVB-light induced late stage skin inflammation. Whereas pro-inflammatory mediators such as TNFα, IL-6 and IL-1β were significantly upregulated in macrophages upon UVB-light exposed lesions in control mice when compared to blood monocytes, expression of these cytokines was significantly reduced in macrophages isolated from IR/IGF-1R[MKO] mice. Interestingly, IL-10 was significantly upregulated in macrophages isolated from UV-light exposed skin in IR/IGF-1R[MKO] mice when compared to controls. Collectively, our findings in IR/IGF-1R[MKO] mice suggest that, during the development of inflammatory skin conditions, IR/IGF-1R activation in macrophages serves to sustain and prolong the cutaneous inflammatory response. Consistently, leukocyte infiltration in control and mutant mice during the early phase of SDS-induced dermatitis as well as in thioglycolate-induced peritonitis, suggest that leukocyte migration or chemotaxis is not affected by IR/IGF-1R-deficiency and thus does not play a primary causative role for attenuated leukocyte influx in late stage inflammation.

The pro-inflammatory function of Insulin/IGF-1 in macrophages that we observed *in vivo* was corroborated by *in vitro* analysis and is consistent with previous reports (4, 5, 19). Of note, stimulation of macrophages by Insulin/IGF-1 *in vitro* led to an induction of the immunosuppressant IL-10, that we however did not detect in macrophages isolated from SDS or UV-light exposed skin lesions in control mice. Rather, we detected a significant upregulation of IL-10 in macrophages isolated from UV-light exposed skin in IR/

IGF-1R[MKO] mice that could contribute to the attenuated late stage inflammatory response observed in UV-light exposed IR/IGF-1R[MKO] mice.

Insulin/IGF-1 stimulation of macrophages *in vitro* resulted in the activation of Akt and p38α and might mediate the identified pro-inflammatory gene expression profiles of monocytes/macrophages and corresponding cutaneous inflammatory responses. Unexpectedly, Insulin/IGF-1 stimulation did not result in activation of mTOR phosphorylation which has been identified as a central downstream target of IR/IGF-1R signaling in diverse cell types (36).

Collectively, our findings demonstrate a direct role for IR/IGF-1R in myeloid cell function that determines innate immune functions of the skin. The different outcomes between the acute wound healing response versus the prolonged *in vivo* stress responses tested in this study suggest that IR/IGF-1R signaling in myeloid cells contributes to perpetuate a local inflammatory response and may contribute to its chronification. The cross-talk between myeloid cells and the epidermal compartment plays an important role in this process. In addition, our findings point towards a critical role of myeloid cell-restricted IR/IGF-1R signalling as an important pathophysiological link between systemic insulin resistant DM and associated cutaneous inflammation. Consistent with this hypothesis is the emerging evidence that systemic immunosuppressive drugs as e.g. TNF inhibitors meliorate both the risk of DM and its associated inflammatory skin diseases including psoriasis (37, 38). Therefore, blocking IR/IGF-1R activation or downstream effectors of this signalling cascade in macrophages, and/or other myeloid cell types, may offer a site for pharmaceutical intervention to inhibit uncontrolled skin inflammatory responses that may arise from systemic inflammatory conditions.

Supplementary Material

Refer to Web version on PubMed Central for supplementary material.

Acknowledgements

Nonstandard abbreviations used in this paper

DM   diabetes mellitus

IGF-1R   insulin-like growth factor 1 receptor
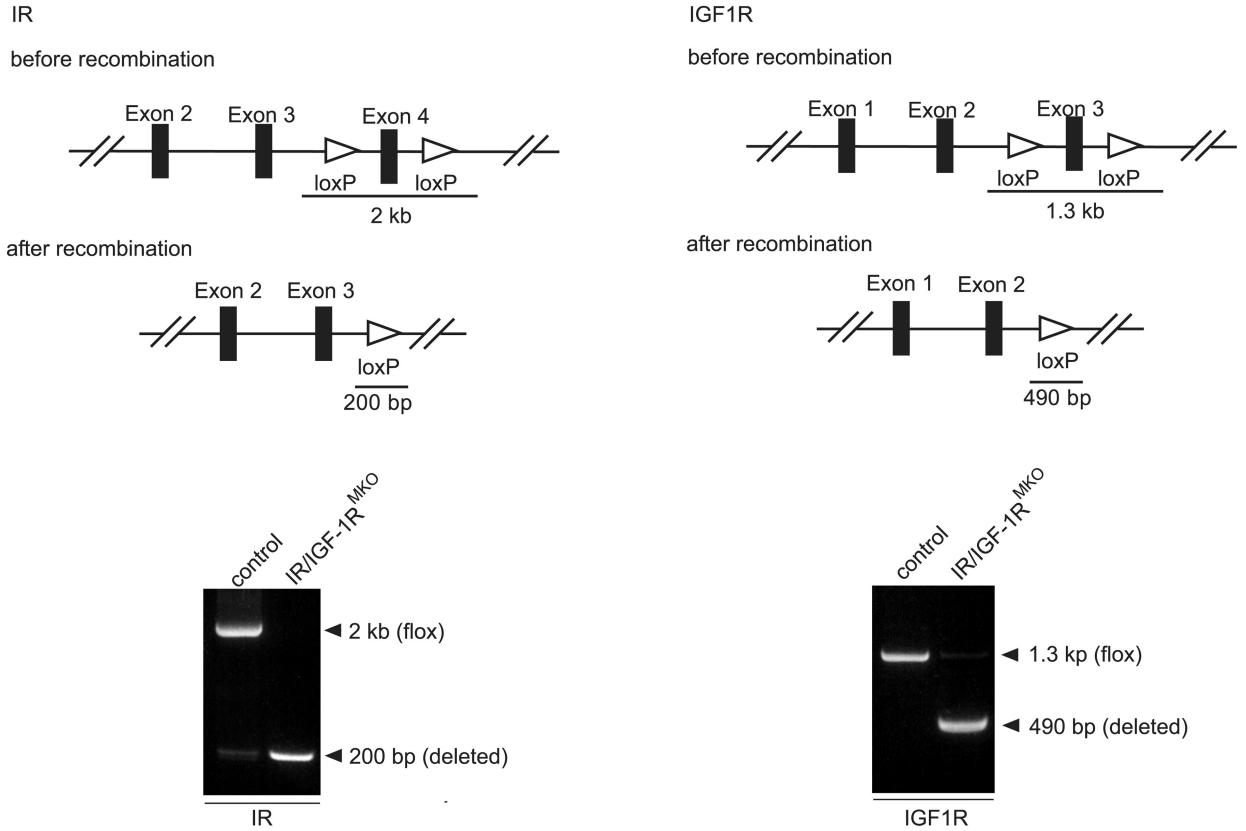
IR   insulin receptor

References

1. McNelis JC, Olefsky JM. Macrophages, Immunity, and Metabolic Disease. Immunity. 2014; 1:36–48. [PubMed: 25035952]

2. Woodcock KJ, Kierdorf K, Pouchelon CA, Vivancos V, Dionne MS, Geissmann F. Macrophage-derived upd3 cytokine causes impaired glucose homeostasis and reduced lifespan in Drosophila fed a lipid-rich diet. Immunity. 2015; 42:133–144. [PubMed: 25601202]

3. Lavin Y, Winter D, Blecher-Gonen R, David E, Keren-Shaul H, Merad M, Jung S, Amit I. Tissue-Resident Macrophage Enhancer Landscapes Are Shaped by the Local Microenvironment. Cell. 2014; 159:1312–1326. [PubMed: 25480296]

4. Baumgartl J, Baudler S, Scherner M, Babaev V, Makowski L, Suttles J, McDuffie M, Tobe K, Kadowaki T, Fazio S, Kahn CR, Hotamisligil GS, Krone W, Linton M, Brüning JC. Myeloid lineage cell-restricted insulin resistance protects apolipoproteinE-deficient mice against atherosclerosis. Cell. Metab. 2006; 3:247–256. [PubMed: 16581002]

5. Mauer J, Chaurasia B, Plum L, Quast T, Hampel B, Blüher M, Kolanus W, Kahn CR, Brüning JC. Myeloid cell-restricted insulin receptor deficiency protects against obesity-induced inflammation and systemic insulin resistance. PLoS Genet. 2010; 6(5):e1000938. [PubMed: 20463885]

6. Nolan CJ, Damm P, Prentki M. Type 2 diabetes across generations: from pathophysiology to prevention and management. Lancet. 2011; 378:169–181. [PubMed: 21705072]

7. Falanga V. Wound healing and its impairment in the diabetic foot. Lancet. 2005; 366:1736–1743. [PubMed: 16291068]

8. Duff M, Demidova O, Blackburn S, Shubrook J. Cutaneous manifestations of diabetes mellitus. Clin. Diabetes. 2015; 33:40–48. [PubMed: 25653473]

9. Demirseren DD, Emre S, Akoglu G, Arpacı D, Arman A, Metin A, Cakır B. Relationship between skin diseases and extracutaneous complications of diabetes mellitus: clinical analysis of 750 patients. Am. J. Clin. Dermatol. 2014; 15:65–70. [PubMed: 24135944]

10. Brownlee M. Biochemistry and molecular cell biology of diabetic complications. Nature. 2001; 414:813–820. [PubMed: 11742414]

11. Baker J, Liu JP, Robertson EJ, Efstratiadis A. Role of insulin-like growth factors in embryonic and postnatal growth. Cell. 1993; 75:73–82. [PubMed: 8402902]

12. Stachelscheid H, Ibrahim H, Koch L, Schmitz A, Tscharntke M, Wunderlich FT, Scott J, Michels C, Wickenhauser C, Haase I, Brüning JC, Niessen CM. Epidermal insulin/IGF-1 signalling control interfollicular morphogenesis and proliferative potential through Rac activation. EMBO J. 2008; 27:2091–2101. [PubMed: 18650937]

13. Günschmann C, Stachelscheid H, Akyüz MD, Schmitz A, Missero C, Brüning JC, Niessen CM. Insulin/IGF-1 controls epidermal morphogenesis via regulation of FoxO-mediated p63 inhibition. Dev. Cell. 2013; 26:176–187. [PubMed: 23906066]

14. Aghdam SY, Eming SA, Willenborg S, Neuhaus B, Niessen CM, Partridge L, Krieg T, Brüning JC. Vascular endothelial insulin/IGF-1 signaling controls skin wound vascularization. Biochem. Biophys. Res. Commun. 2012; 421:197–202. [PubMed: 22503682]

15. Roth D, Piekarek M, Christ H, Paulsson M, Bloch W, Krieg T, Davidson J, Eming SA. Plasmin modulates VEGF-A mediated angiogenesis during wound repair. Am. J. Pathol. 2006; 168:670–684. [PubMed: 16436680]

16. Hoffmann DC, Willenborg S, Koch M, Zwolanek D, Müller S, Becker AK, Metzger S, Ehrbar M, Kurschat P, Hellmich M, Hubbell JA, Eming SA. Proteolytic processing regulates placental growth factor activities. J. Biol. Chem. 2013; 288:17976–17989. [PubMed: 23645683]

17. Bar RS, Gorden P, Roth J, Kahn CR, De Meyts P. Fluctuations in the affinity and concentration of insulin receptors on circulating monocytes of obese patients: effects of starvation, refeeding, and dieting. J. Clin. Invest. 1976; 58:1123–1135. [PubMed: 993336]

18. Costa Rosa LFBP, Safi DA, Cury Y, Curi R. The effect of Insulin on Macrophage Metabolism and Function. Cell Biochem. Funct. 1996; 14:33–42. [PubMed: 8907252]

19. Renier G, Clément I, Desfaits AC, Lambert A. Direct stimulatory effect of insulin-like growth factor-I on monocyte and macrophage tumor necrosis factor-alpha production. Endocrinology. 1996; 137:4611–4618. [PubMed: 8895324]

20. Nakae J, Kido Y, Accili D. Distinct and overlapping functions of insulin and IGF-I receptors. Endocr. Rev. 2001; 22:818–835. [PubMed: 11739335]

21. White MF. Insulin signaling in health and disease. Science. 2003; 302:1710–1711. [PubMed: 14657487]

22. Brüning JC, Michael MD, Winnay JN, Hayashi T, Hörsch D, Accili D, Goodyear LJ, Kahn CR. A muscle-specific insulin receptor knockout exhibits features of the metabolic syndrome of NIDDM without altering glucose tolerance. Mol. Cell. 1998; 2:559–569. [PubMed: 9844629]

23. Clausen BE, Burkhardt C, Reith W, Renkawitz R, Förster I. Conditional gene targeting in macrophages and granulocytes using LysMcre mice. Transgenic Res. 1999; 8:265–277. [PubMed: 10621974]

24. Kim C, Sano Y, Todorova K, Carlson BA, Arpa L, Celada A, Lawrence T, Otsu K, Brissette JL, Arthur JS, Park JM. The kinase p38 alpha serves cell type-specific inflammatory functions in skin injury and coordinates pro- and anti-inflammatory gene expression. Nat. Immunol. 2008; 9:1019–1027. [PubMed: 18677317]

25. Thepen T, van Vuuren HAJ, Kiekens RCM, Damen CA, Vooijs WC, van de Winkel JGJ. Resolution of cutaneous inflammation after local elimination of macrophages. Nat. Biotechnol. 2000; 18:48–51. [PubMed: 10625390]

26. Cramer T, Yamanishi Y, Clausen BE, Förster I, Pawlinski R, Mackman N, Haase VH, Jaenisch R, Corr M, Nizet V, Firestein GS, Gerber HP, Ferrara N, Johnson RS. HIF-1α is essential for myeloid cell-mediated inflammation. Cell. 2003; 5:645–657. [PubMed: 12628185]

27. Cela EM, Friedrich A, Paz ML, Vanzulli SI, Leoni J, Magoli D. H. Gonzalez. Time-course study of different innate immune mediators produced by UV-irradiated skin. Immunology. 2014; 145:82–93. [PubMed: 25438991]

28. Wicks K, Torbica T, Mace KA. Myeloid cell dysfunction and the pathogenesis of the diabetic chronic wound. Semin. Immunol. 2014; 26:341–353. [PubMed: 24954378]

29. Seitz O, Schürmann C, Hermes N, Müller E, Pfeilschifter J, Frank S, Goren I. Wound Healing in Mice with High-Fat Diet- or ob Gene-Induced Diabetes-Obesity Syndromes: A Comparative Study. Exp. Diabetes Res. 2010:476969. [PubMed: 21318183]

30. Wood S, Jayaraman V, Huelsmann EJ, Bonish B, Burgad D, Sivaramakrishnan G, Qin S, DiPietro LA, Zloza A, Zhang C, Shafikhani SH. Pro-Inflammatory Chemokine CCL2 (MCP-1) Promotes Healing in Diabetic Wounds by Restoring the Macrophage Response. PLoS ONE. 2014; 9(3):e91574. [PubMed: 24618995]

31. Lucas T, Waisman A, Ranjan R, Roes J, Krieg T, Müller W, Roers A, Eming SA. Differential roles of macrophages in diverse phases of skin repair. J. Immunol. 2010; 184:3964–3977. [PubMed: 20176743]

32. Willenborg S, Lucas T, van Loo G, Knipper JA, Krieg T, Haase I, Brachvogel B, Hammerschmidt M, Nagy A, Ferrara N, Pasparakis M, Eming SA. CCR2 recruits an inflammatory macrophage subpopulation critical for angiogenesis in tissue repair. Blood. 2012; 120:613–625. [PubMed: 22577176]

33. Selman C, Lingard S, Choudhury AI, Batterham RL, Claret M, Clements M, Ramadani F, Okkenhaug K, Schuster E, Blanc E, Piper MD, Al-Qassab H, Speakman JR, Carmignac D, Robinson IC, Thornton JM, Gems D, Partridge L, Withers DJ. Evidence for lifespan extension and delayed age-related biomarkers in insulin receptor substrate 1 null mice. FASEB J. 2008; 22:807–818. [PubMed: 17928362]

34. Nair MG, Du Y, Perrigoue JG, Zaph C, Taylor JJ, Goldschmidt M, Swain GP, Yancopoulos GD, Valenzuela DM, Murphy A, Karow M, Stevens S, Pearce EJ, Artis D. Alternatively activated macrophage-derived RELM-α is a negative regulator of type 2 inflammation in the lung. J. Exp. Med. 2009; 206:937–952. [PubMed: 19349464]

35. Pesce JT, Ramalingam TR, Wilson MS, Mentink-Kane MM, Thompson RW, Cheever AW, Urban JF Jr, Wynn TA. Retnla (relmα/fizz1) suppresses helminth-induced Th2-type immunity. PLoS Pathogens. 2009; 5(4):e1000393. [PubMed: 19381262]

36. Wullschleger S, Loewith R, Hall MN. TOR signaling in growth and metabolism. Cell. 2006; 124:471–484. [PubMed: 16469695]

37. Solomon DH, Massarotti E, Garg R, Liu J, Canning C, Schneeweiss S. Association between disease-modifying antirheumatic drugs and diabetes risk in patients with rheumatoid arthritis and psoriasis. JAMA. 2011; 305:2525–2531. [PubMed: 21693740]

38. Armstrong AW, Harskamp CT, Armstrong EJ. Psoriasis and the risk of diabetes mellitus: a systematic review and meta-analysis. JAMA Dermatol. 2013; 149:84–91. [PubMed: 23407990]

A

IR

before recombination

IGF1R

before recombination

after recombination

after recombination

B

Figure 1. Conditional targeting of the IR and IGF-1R gene
(A) Top, scheme illustrating the IR (left) and IGF-1R (right) gene construct and the 2 loxP sites flanking exon 4 (IR, left) or exon 3 (IGF-1R, right), respectively, and the PCR fragment length shown before and after successful recombination. Bottom, PCR analysis on genomic DNA isolated from peritoneal macrophages of control (IR^{fl/fl}/IGF-1R^{fl/fl}) and IR/IGF-1R[MKO] mice showing the deletion of the floxed region in the IR (left) and IGF-1R (right) locus in the presence of LysM-driven Cre. (B) Western blot analysis for IR (left) and IGF-1R (right) of peritoneal macrophages isolated from control or IR/IGF-1R[MKO] mice as indicated.
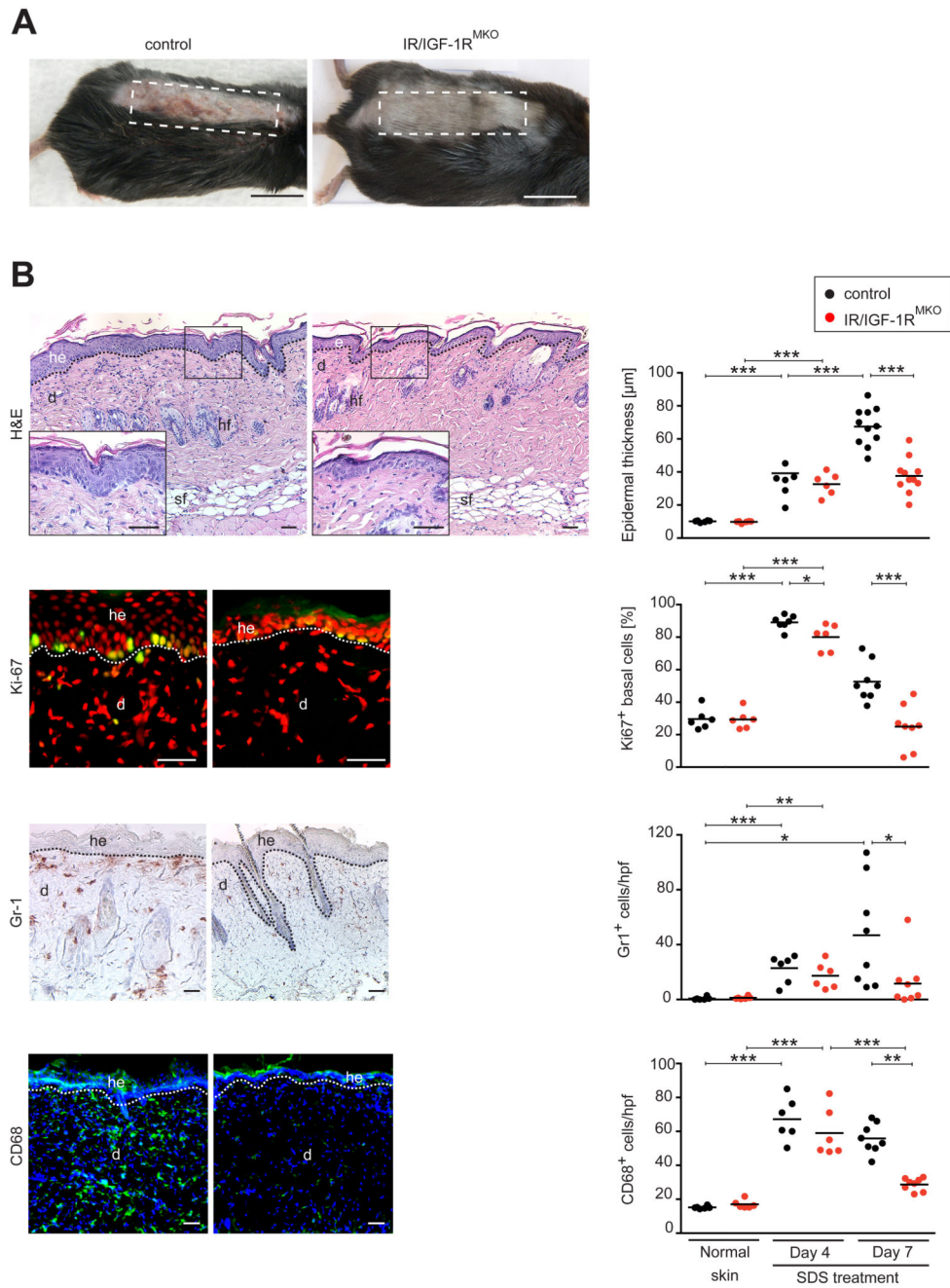
Figure 2. Myeloid cell-specific IR/IGF-1R deficiency protects against SDS-induced skin inflammation

(A) Macroscopic appearance of control and IR/IGF-1R^MKO mice 7 days after SDS application; dashed line outlines treated area; scale bars indicate 1 cm. (B) Representative histological sections (left panel) and quantitative analysis of epidermal thickness and cells within skin lesions (right panel) at indicated time points post SDS treatment: H&E staining, Ki67 (Ki67+ cells green, counter stain propidium iodide), Gr-1 (Gr-1+ cells brown, heamatoxylin counter stain), CD68 (CD68+ cells green, counter stain DAPI); each dot represents one mouse; scale bars indicate 40 μm; he=hyperproliferative epidermis, d=dermis,

sf=subcutaneous fat layer, hf=hair follicle; * p-value <0.05, ** p-value <0.01, *** p-value <0.001.
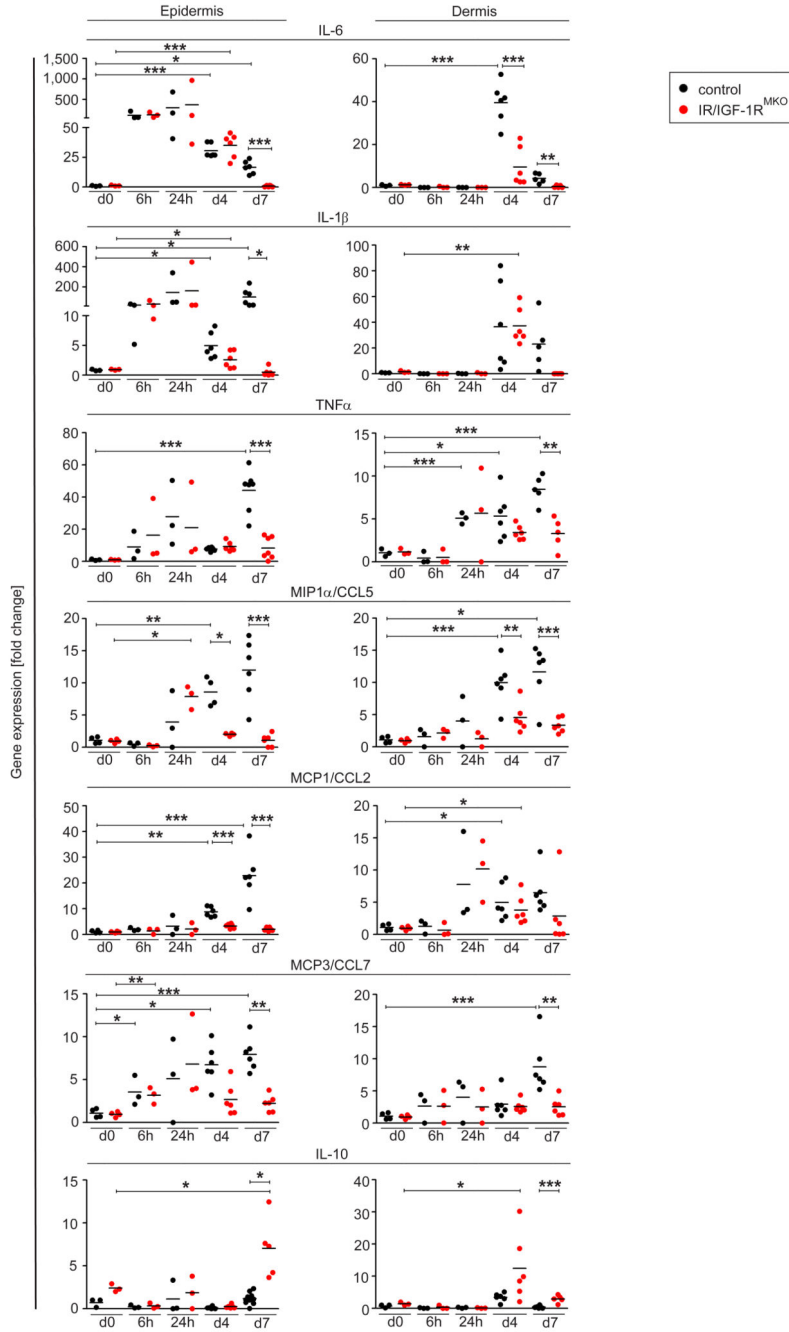
Figure 3. Myeloid cell-specific IR/IGF-1R deficient mice show decreased expression of inflammatory mediators in SDS-treated skin

qRT-PCR analysis of selected genes in epidermal or dermal tissues of untreated skin or at different time points after SDS treatment as indicated; each dot represents one mouse. * p-value <0.05, ** p-value <0.01, *** p-value <0.001.
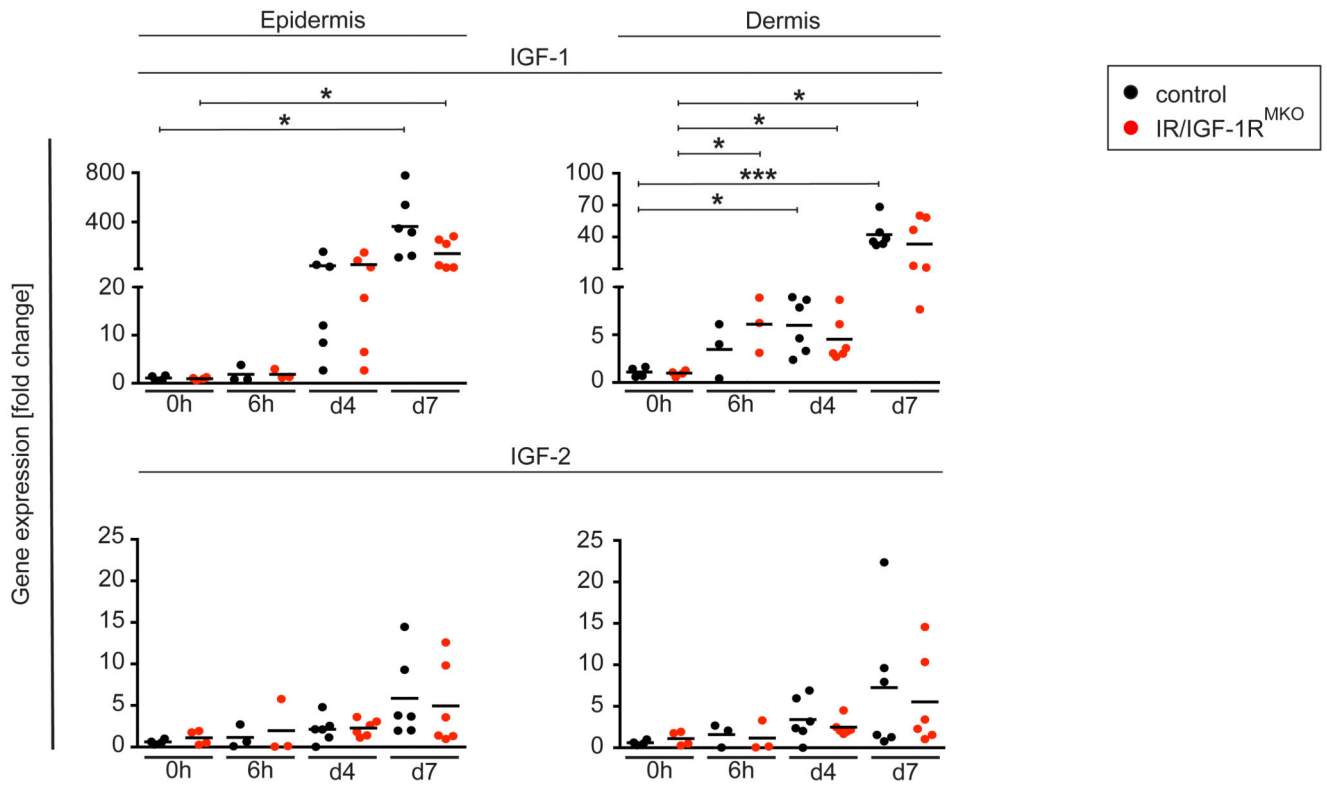
Figure 4. IGF-1/-2 expression in SDS-treated skin

qRT-PCR analysis of IGF-1 and IGF-2 genes in epidermal or dermal tissues of untreated skin or at different time points after SDS treatment as indicated; each dot represents one mouse. * p-value <0.05, *** p-value <0.001.
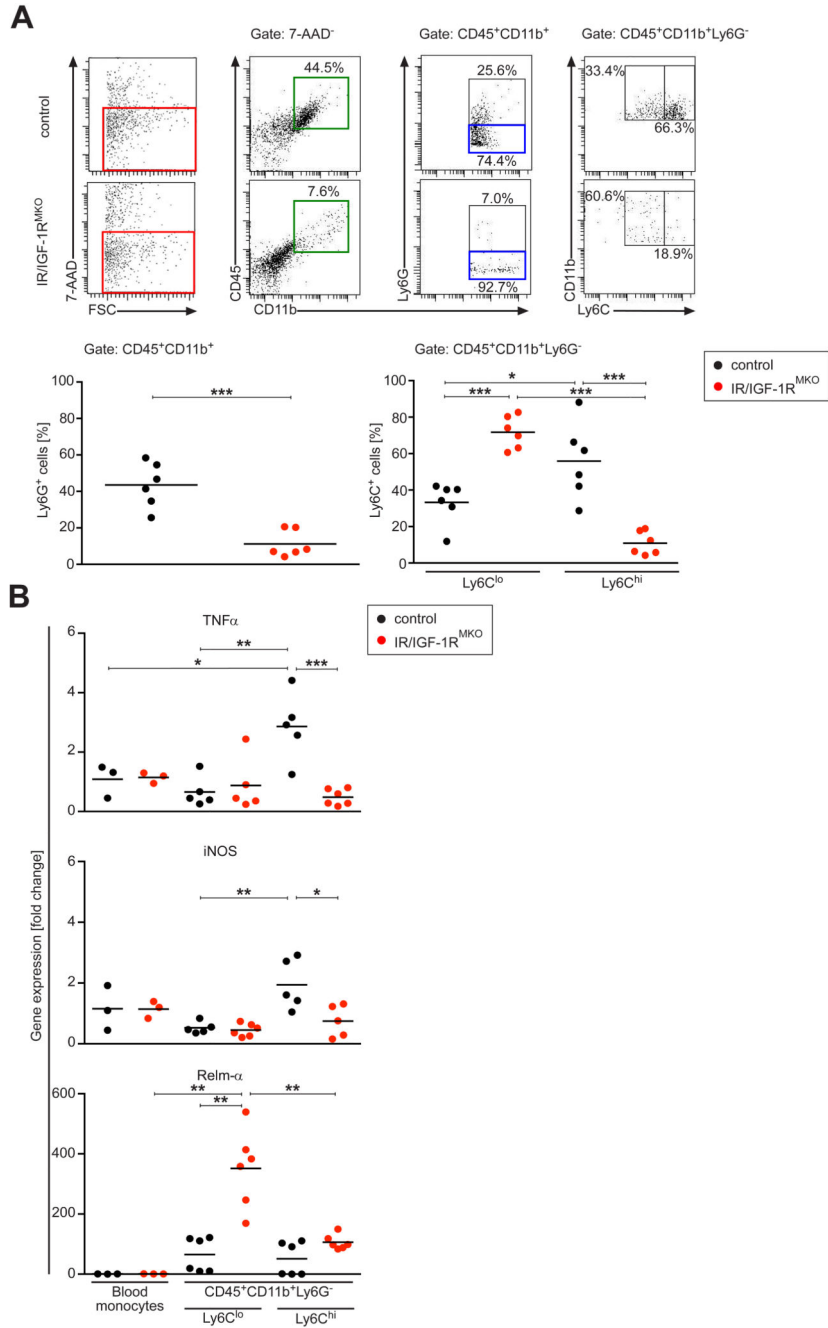
Figure 5. Myeloid cell-specific IR/IGF-1R expression controls macrophage activation
(A) Top, representative FACS analysis of single-cell suspensions of SDS-treated skin at day 7. Bottom, 7-AAD⁻ cells (red square) were gated and analysed for expression of CD45, CD11b, Ly6G and Ly6C as indicated and quantified. (B) qRT-PCR of selected genes in CD45+CD11b+Ly6G−Ly6C^hi and CD45+CD11b+Ly6G−Ly6C^lo FACS sorted cells of the SDS-treated tissue, normalized to SSC^low CD11b+CD115+ blood monocytes; each dot represents one mouse. * p-value <0.05, ** p-value <0.01, *** p-value <0.001.
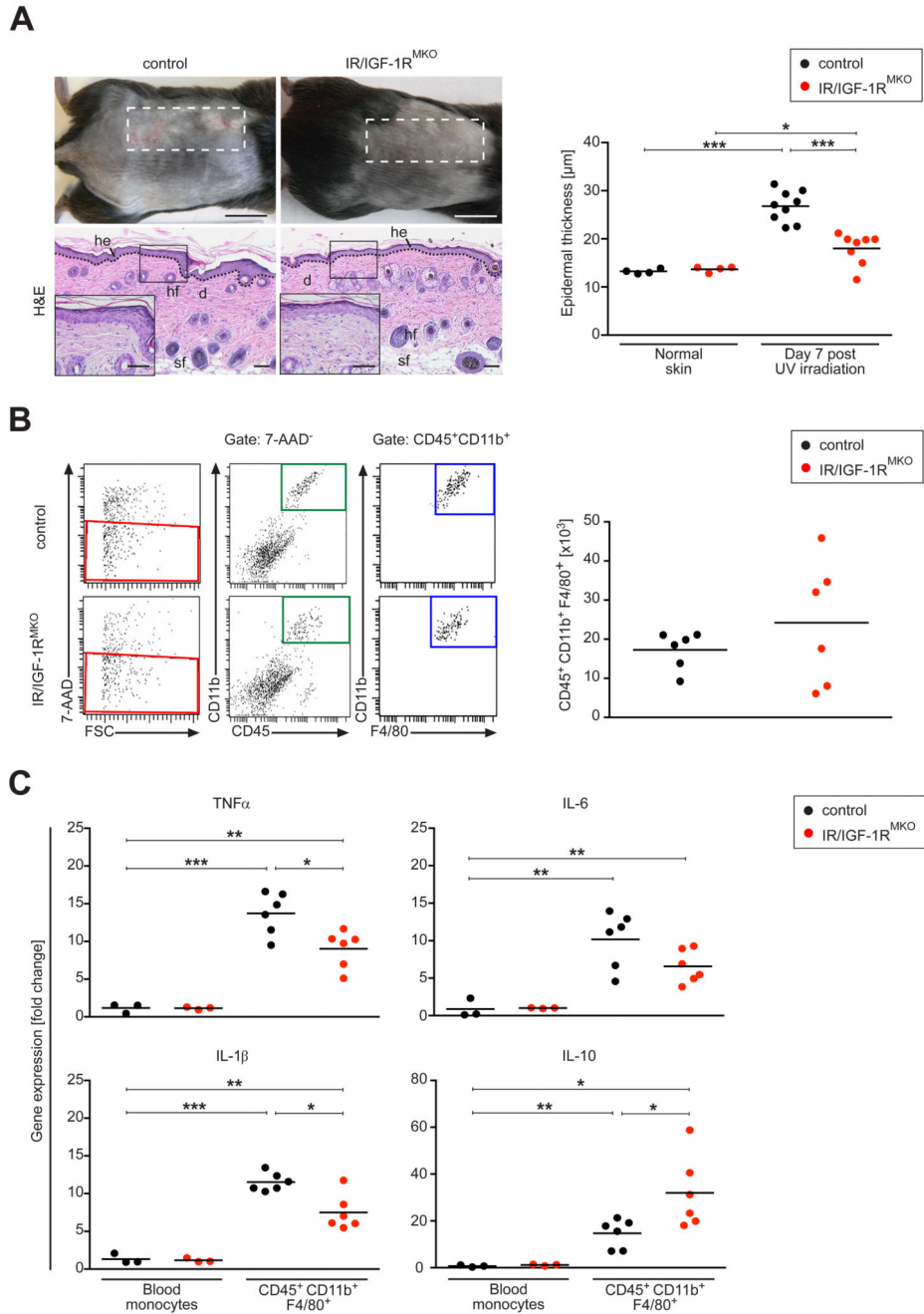
Figure 6. Myeloid cell-specific IR/IGF-1R deficiency protects from UVB-induced skin inflammation

(A) Representative macroscopic appearance (top) and histology (bottom, H&E stain) of skin 7 days after UVB irradiation; dashed line outlines irradiated area; right panel, quantification of epidermal thickness; each dot represents one mouse; scale bars indicate 1 cm. (B) Left, representative FACS analysis of single-cell suspensions of UVB-irradiated skin at day 7; right, 7-AAD$^-$ cells (red square) were gated and analysed for expression of CD45, CD11b, F4/80 and quantified. (C) qRT-PCR of selected genes in CD45$^+$CD11b$^+$F4/80$^+$ FACS sorted

cells of the UVB-irradiated tissue, normalized to $SSC^{low}CD11b^{+}CD115^{+}$ blood monocytes; each dot represents one mouse. * p-value <0.05, ** p-value <0.01, *** p-value <0.001.
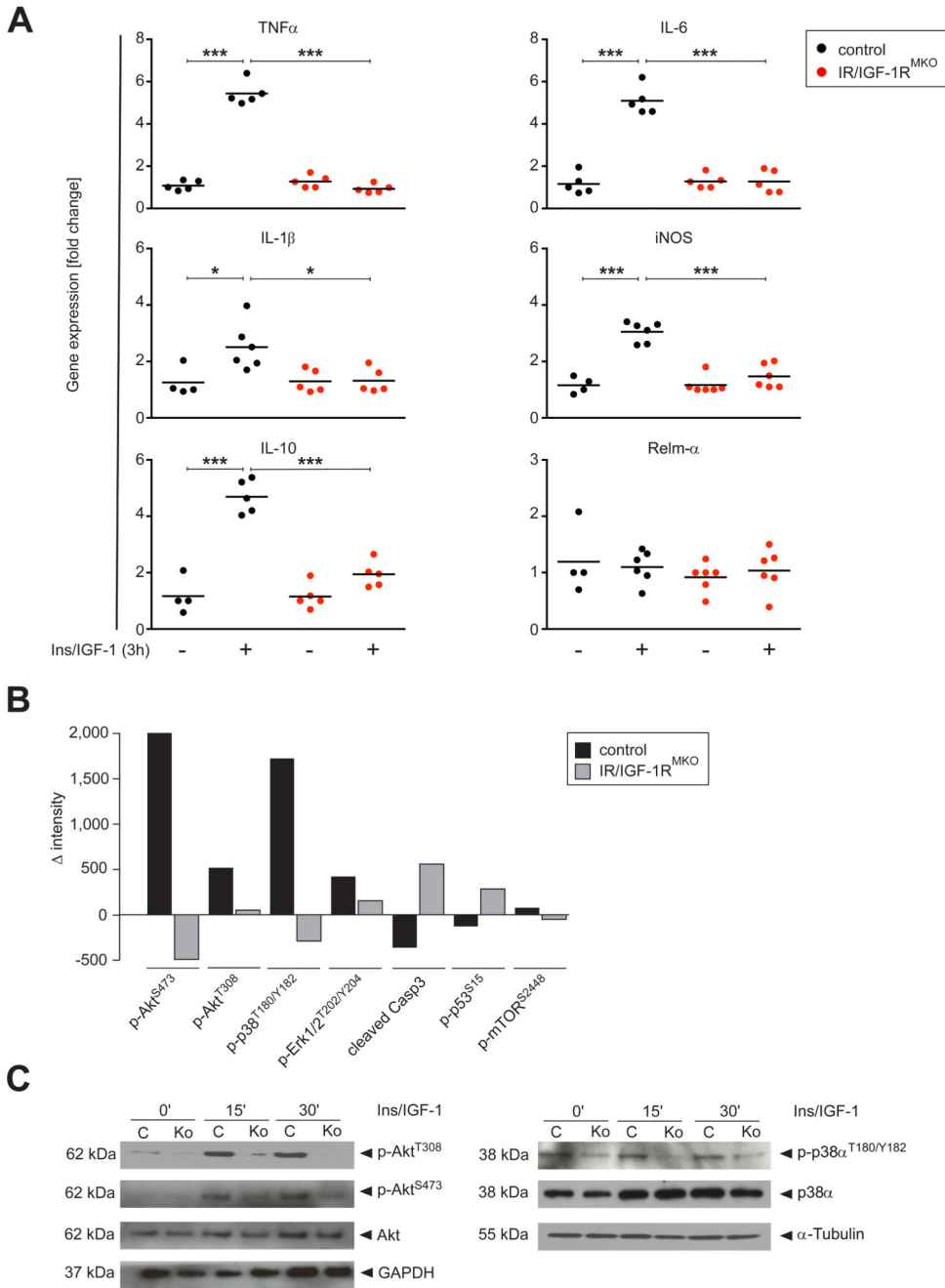
Figure 7. Insulin and IGF-1 induce a pro-inflammatory macrophage phenotype *in vitro* associated with activation of Akt and p38α MAPK

(A) qRT-PCR analysis of selected genes in peritoneal macrophages cultured in the presence of a combination of rInsulin and rIGF-1 (+) or vehicle (−) for 3 h; gene expression in rInsulin/rIGF-1 stimulated cells is normalized to vehicle treated cells; each dot represents macrophages isolated from one mouse; * p-value <0.05, *** p-value <0.001. (B) PathScan® Intracellular Signaling Array Kit analysis of peritoneal macrophages isolated from control and IR/IGF1R[MKO] mice cultured for 15 min in rInsulin/rIGF-1 or vehicle; presented is the difference of chemiluminescent intensity of selected phosphorylated proteins between

rInsulin/rIGF-1 stimulated or vehicle treated cells; presented is the mean of 2 independent experiments. (C) Western blot analysis for p-Akt and p-p38α of peritoneal macrophages, stimulated for indicated time periods with rInsulin/rIGF-1; C=control mice, Ko=IR/IGF-1R^{MKO} mice; α-Tubulin and GAPDH served as loading controls.
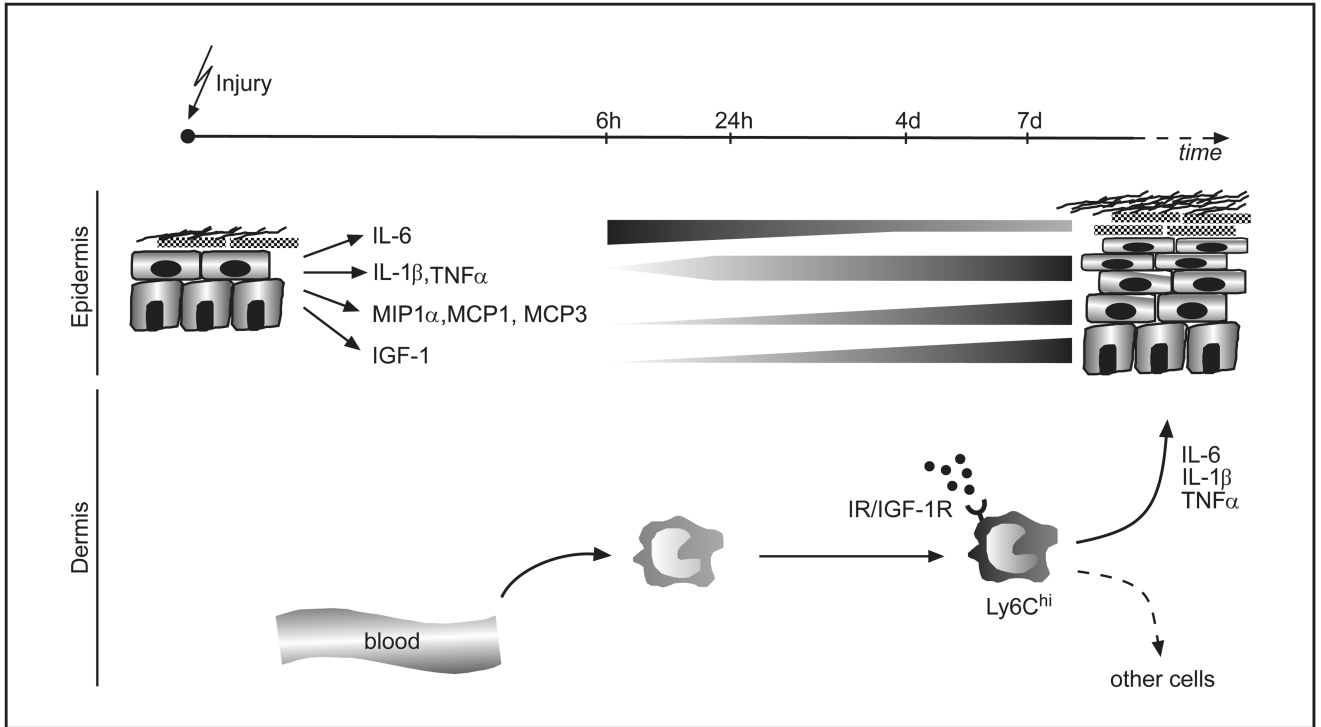
Figure 8. Hypothetical model of myeloid cell-restricted IR/IGF-1R function in the dynamics of the epidermal-dermal crosstalk in skin inflammation

Epidermal injury causes rapid release of pro-inflammatory mediators (IL-6, IL-1β, TNFα) and chemokines (MIP1α, MCP1, MCP3) that mediate effective recruitment of blood monocytes/macrophages into the dermis; influx of myeloid cells during the early phase of inflammation appears independent of myeloid cell-restricted IR/IGF1-R; during late stage inflammation, myeloid cell-restricted IR/IGF1-R activation induces a pro-inflammatory macrophage phenotype that sustains epidermal inflammation by the release of pro-inflammatory mediators (IL-6, IL-1β, TNFα).